NOAA Contract Report NMFS-NWFSC-CR-2023-01

https://doi.org/10.25923/xf8y-x065

Habitat Capacity for Chinook Salmon and Steelhead Spawning and Rearing in the Similkameen River Basin

Contract **TU-2021-01**

January 2023

U.S. DEPARTMENT OF COMMERCE

National Oceanic and Atmospheric Administration
National Marine Fisheries Service
Northwest Fisheries Science Center

NOAA Contract Report Series NMFS-NWFSC-CR

Recommended citation:

(Bond et al. 2023)[1]

[1] Bond, M. H., T. J. Beechie, and G. R. Pess. 2023. Habitat Capacity for Chinook Salmon and Steelhead Spawning and Rearing in the Similkameen River Basin. U.S. Department of Commerce, NOAA Contract Report NMFS-NWFSC-CR-2023-01.

https://doi.org/10.25923/xf8y-x065

Habitat Capacity for Chinook Salmon and Steelhead Spawning and Rearing in the Similkameen River Basin

Morgan H. Bond, Timothy J. Beechie, and George R. Pess

https://doi.org/10.25923/xf8y-x065

January 2023

Fish Ecology Division
Northwest Fisheries Science Center
2725 Montlake Boulevard East
Seattle, Washington 98112

U.S. DEPARTMENT OF COMMERCE

National Oceanic and Atmospheric Administration
National Marine Fisheries Service
Northwest Fisheries Science Center

Table of Contents

Acknowledgments

This modeling work was substantially improved through the advice and contributions of Oleksandr Stefankiv, Colin Nicol, and Jeff Jorgensen. Invaluable field data were collected by Chris Fisher of the Confederated Tribes of the Colville Reservation, the Lower Similkameen Band of Indians, and the Upper Similkameen Band of Indians. We also thank the National Geospatial Intelligence Agency for access to satellite imagery.

Executive Summary

We conducted a geomorphic analysis of potential salmon habitat in the basin, assuming unimpaired passage of Chinook salmon (*Oncorhynchus tshawytscha*), and steelhead (*Oncorhynchus mykiss*) into the mainstem Similkameen River past Coyote Falls and the Enloe Dam site. The Similkameen River has been inaccessible to anadromous fish since 1922, when Enloe Dam was constructed at river kilometer 14. We determined the anadromous extent of the basin with a combination of ground survey barrier identification from the Upper and Lower Similkameen Tribes, and maximum accessible stream gradients derived from topographic information (Canada 20 m DEM and LiDAR 1 m), resulting in 2446 km of accessible habitat out of all 5504 km of streams in our Similkameen River Basin dataset. We used catchment area and average annual precipitation of each reach to estimate stream size and a total average wetted habitat area of 2193 hectares. We estimated spawning gravel areas for each species based on stream slope and pool spacing. The spawning habitat divided by average redd area indicated a redd capacity of 80,705 and 210,729 for Chinook salmon and steelhead, respectively. In addition, we estimated juvenile rearing habitats in large rivers (large stream banks, bars, mid-channel, and side channel), and smaller streams (pools and riffles). For each estimated habitat type area, we applied literature-derived parr densities to estimate a total parr rearing habitat capacity of 6,645,841 and 10,252,583 for Chinook salmon and steelhead, respectively. Applying an average parr to smolt survival for each species, we estimate parr at capacity would result in ca. 1.5 million Chinook smolts and 2.9 million steelhead smolts, similar to previous estimates for the Similkameen River. At recent smolt to adult survival rates for the Upper Columbia, smolt abundances of these magnitudes would likely result in ca. 7,800-47,000 Chinook salmon spawners, and 29,500-118,300 steelhead spawners returning to the Similkameen River.

Introduction

The Similkameen River, Okanogan River's largest tributary, has been almost entirely inaccessible to anadromous fishes since the completion of Enloe Dam (rkm 14) in 1922. With a watershed area of 9270 km^2, the Similkameen River has a considerable amount of habitat that cannot currently be accessed by anadromous fishes; it is the largest sub-basin in the Pacific Northwest that is currently blocked by a relict dam. Moreover, with the removal of Enloe Dam, the Similkameen River would become accessible to two species of salmonids listed as threatened (Upper Columbia River Steelhead, *Oncorhynchus mykiss*), and endangered (Upper Columbia River Spring-run Chinook Salmon, *Oncorhynchus tshawytscha*), in the Upper Columbia Evolutionarily Significant Unit under the Endangered Species Act. Historical records of salmon use of the Similkameen River are scant because of the age of the dam, and there is some debate about access above Coyote Falls (aka Enloe Falls, Similkameen Falls) just below the dam site. For the purposes of this study we assume that following dam removal, the river above the dam and falls would become accessible to spring and/or summer-run Chinook salmon and steelhead as both species inhabit the Okanogan River, into which the Similkameen River feeds, and the nearby Methow River.

Salmon have not inhabited the Similkameen River above the Enloe dam site for a century. Therefore, to estimate the benefits of habitat access for anadromous fishes, we used information gleaned from decades of research in other similar Pacific Northwest streams currently occupied by salmon and steelhead. Our initial analysis takes a geomorphic approach to estimating the spawning and rearing capacity of the Similkameen River Basin above Enloe Dam. That is, we used topography, precipitation, and land use to estimate the most likely habitat types in each stream reach and their size. To each habitat type we apply species-specific documented maximum densities of juveniles and spawners, which are summed within and across habitat types to calculate a total capacity. Although the availability of data to populate these habitat expansion models varies regionally, this general approach has been used in many Pacific Northwest rivers and streams (Bartz et al. 2006; Beechie et al. 2021; Bond et al. 2019). This approach is particularly useful in locations like the Similkameen where there are currently no or few anadromous fishes to survey for local habitat use. Our objectives were to: 1. Estimate rearing capacity for the first summer parr life stage for both Chinook salmon and steelhead, and 2. Estimate spawning habitat capacity for Chinook salmon and steelhead. These estimates provide a reference upon which other management or restoration scenarios or conditions can be layered as more data become available. In a subset of mainstem habitats, we used a more detailed set of topographic data and high resolution satellite imagery to update the geomorphic estimates at important flows relevant to the phenology of each species.

Habitat Modeling - Geomorphic

The geomorphic approach builds a capacity estimate from habitat properties that emerge from two primary sources of data, topography and stream discharge in each stream reach. From these data, we can estimate the basic habitat characteristics that are available to fish for spawning and rearing. The amounts and locations of each of these habitat types determine the overall juvenile rearing and adult spawner capacities of the system.

The US Geological Survey's National Hydrography Dataset (NHDPlus-HR) forms the backbone for all analyses in this project in both the US and Canada (Figure 1). Although NHD stream reach segments vary in length, to facilitate our analyses, we split the entire network into 200 m long reaches, with some reaches smaller than 200 m forming the remainder of a tributary that cannot be divided equally into 200 m segments. Although the NHD network provides some information about where we expect streams to occur on the landscape, characteristics of each reach are primarily derived from basin-wide estimates of topography, hydrography, geology, precipitation, and land use to estimate the discharge, slope, sediment supply, sinuosity, bankfull width, wetted width, and confinement of each stream reach. Slopes and elevations were derived from a basin-wide 10 m digital elevation model (DEM) that was created by merging the U.S. (National Elevation Dataset (NED), 10 m horizontal resolution) and Canadian (Canada Digital Elevation Data (CDED), 20 m horizontal resolution, upsampled to 10m matching NED) elevation datasets. These slopes were updated with a more accurate LiDAR derived DEM (1 m resolution), where those data were available (Figure 2). Bankfull width (BFW) and mean annual discharge (Q_{ave}) were estimated based on DEM-derived drainage area (A) and mean annual precipitation estimates (PRISM, ClimateBC) with the following equation:

Eq 1. $BFW = 0.177 \cdot A^{0.397} \cdot Q_{ave}^{0.453}$

These attributes were used to predict mainstem stream habitat across the basin using a model that relates the variables driving channel planform (e.g. island-braided, meandering, etc.) to a stream's potential for providing high quality fish habitat (Beechie and Imaki 2014; Bond et al. 2017; Bond et al. 2019). We also estimated wetted width (W_w) for each stream segment using a random forest regression with eight predictor variables: current floodplain width, sediment accumulation, discharge, bankfull width, bankfull depth, slope, sinuosity, and elevation (Bond et al. 2019).

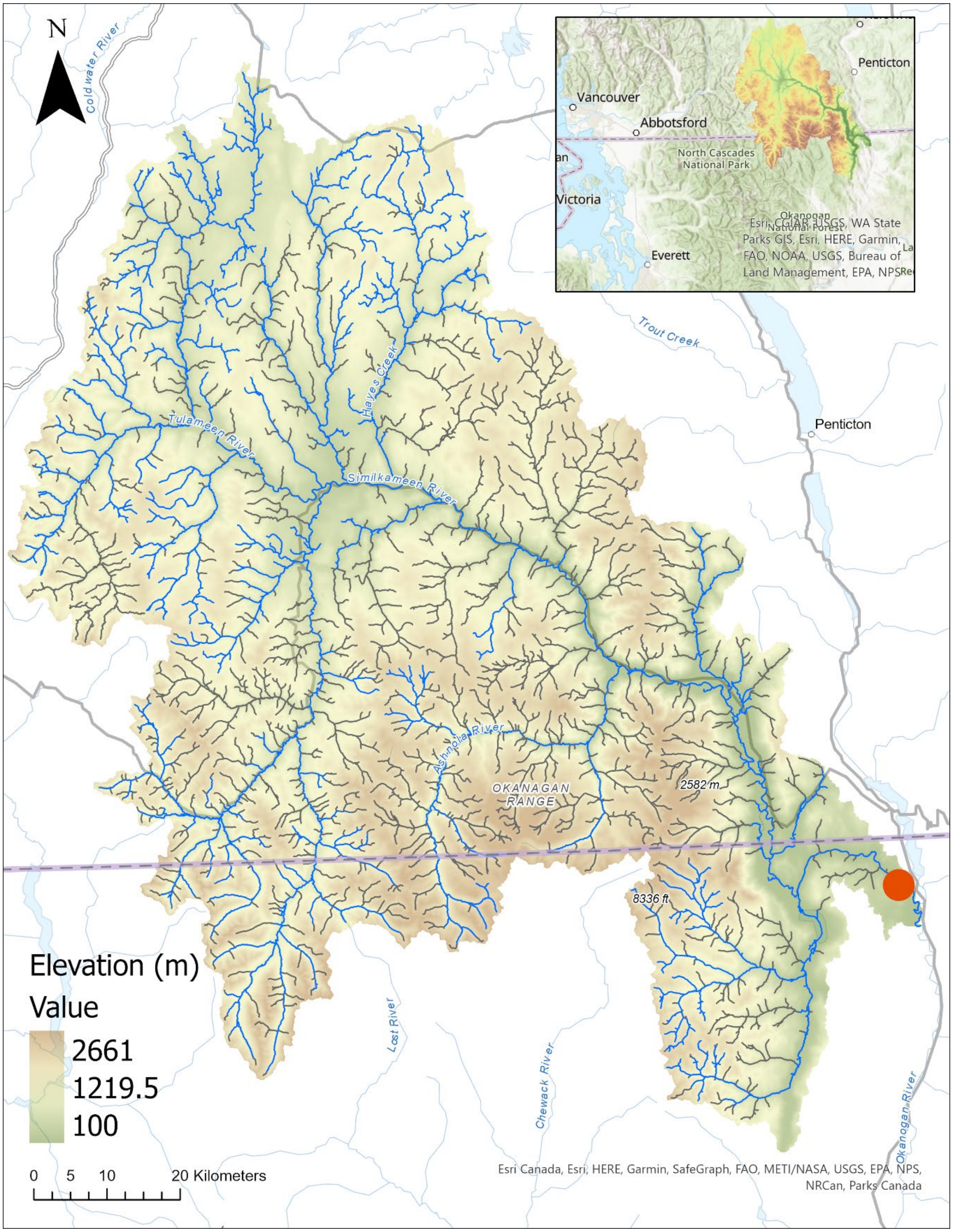

Figure 1. Similkameen River watershed displaying general topography and hydrography. Rivers and streams estimated to be available to anadromous fish in blue and inaccessible streams in gray. The Enloe Dam location (red point) is on the lower Similkameen River just south of the U.S.-Canadian border (dashed pink line).

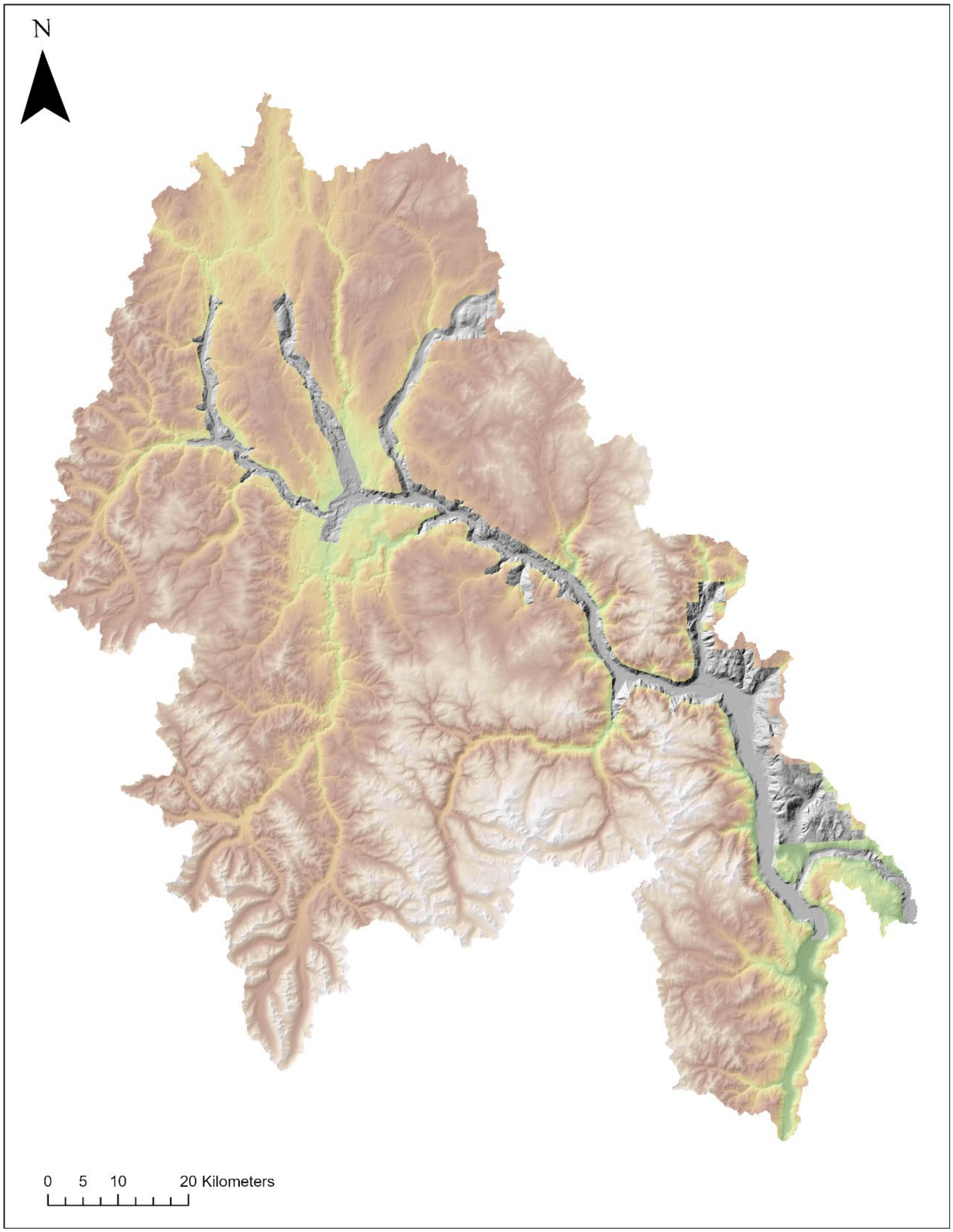

Figure 2. The Similkameen River watershed displaying the combined digital elevation model from the U.S. National Elevation Dataset (10 m horizontal resolution) and the upsampled Canadian Digital Elevation Dataset (20 m horizontal resolution) in color gradient by elevation. LiDAR based digital elevation model mosaic (1 m horizontal resolution) from U.S. and Canadian data in grayscale hillshade.

A key component of developing habitat capacity models is the determination of upstream anadromous extents (Figure 1). In the Similkameen River Basin, there are no established historical anadromous fish distributions. In lieu of these data, we took a multi-step approach to limiting our stream network to the most likely anadromous habitat. First, we removed streams above known large barriers. For example, the ca. 30 m high Tulameen Falls clearly blocks access to the upper Tulameen River. Secondly, we used barriers determined by ground surveys by the Upper and Lower Similkameen Indian Bands biologists. Finally, for streams with no known large barriers or ground survey barriers identified, we used stream slopes derived from LiDAR where available, or from the composite DEM layer (Figure 3). We excluded reaches upstream of three consecutive 200 m reaches exceeding 12% slope, or a single 200 m reach slope exceeding 18%. Typically, these exclusions matched well with the ground survey barrier identification. In addition, late summer ground surveys often identified dry streams, which fell below the minimum 3.6 m estimated bankfull width and were therefore excluded by width. We did not exclude streams where logjams were the only barrier identified during ground surveys, as these are rarely full barriers to migration when slope and discharge requirements for inclusion are met. In previous analyses of fish habitat in the Similkameen River system, several additional areas of potentially difficult passage were identified (DoE 1984), including the lower Ashnola River and Similkameen Falls. Although photo analysis indicated that these are unlikely to be complete barriers, they may provide difficult passage during years of unusually high or low stream flows. For this reason, we have estimated the total system spawning and rearing capacity with and without tributaries that would be blocked by flow-dependent passability in these areas.

In small streams, we estimated pool and riffle area (Table 1) based on channel slope, using the average percent pool for stream segments in forest lands of the Skagit River basin (forest is the dominant land cover type along tributaries in the Similkameen). The average

Table 1. Habitat type definitions for habitats known to be used by juvenile Chinook salmon and steelhead and estimated with geomorphic assessments (Beechie et al. 1994, 2005).

Macro habitat type	Habitat type	Definition
Small stream	Riffle	Shallow, fast water (typically >0.45 m/sec)
	Pool	Deep, slow water (typically <0.45 m/sec)
Large river	Bank edge	Vertical or steeply sloping shore, velocity <0.45 m/sec, depth <1.0 m, no bank armor
	Bar edge	Gently sloping shore, velocity <0.45 m/sec, depth <1.0 m
	Mid-channel	All habitat area not included in bank and backwater habitats, often >1 m deep or velocity >0.45 m/sec
Floodplain	Side Channel	Seasonally inundated channel

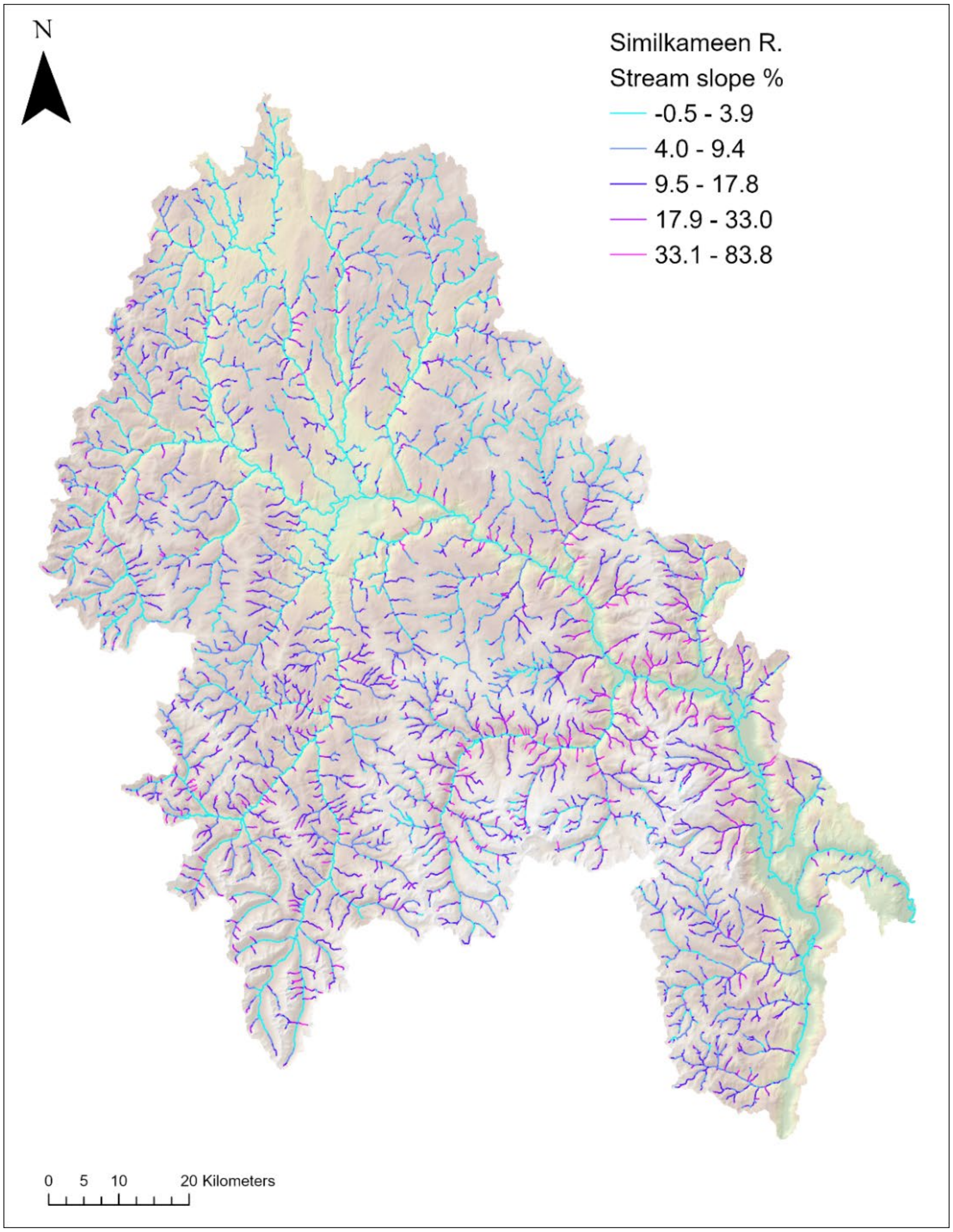

Figure 3. Stream slopes (%) in the Similkameen watershed derived from NED, CDED and LiDAR sources.

percent pool in forest lands in the Skagit River basin was 61% in channels <2% slope, 29% in channels 2-4% slope, and 27% in channels >4% slope (Beechie et al. 2001). We multiplied percent pool in each reach by wetted width to calculate pool area, and riffle area was the remaining wetted area in each reach.

For larger river reaches (> 8 m wide), we estimated bank edge, bar edge, and mid-channel areas (Figure 4), as well as the side channel area (Table 1). The side channel area in each reach was estimated following the methods of Bond et al. (2019). Random forest classification and regression models predicting side channel habitat were constructed from measurements of side channels throughout the Columbia River Basin (CRB) and previously derived stream characteristics for each reach. Similarly, the bank edge and bar edge area in each reach was derived from a random forest model of measured bank and bar edge lengths at 70 locations throughout the CRB. To estimate usable bank and bar edge habitat area we used regressions of bar edge (Eq 2.) and bank edge (Eq 3.) width on total stream width developed from measurements of the Chehalis River in Washington State (Tim Beechie, unpublished data):

Eq 2. $W_{bar} = 0.0872 \times W_w + 2.114$

Eq 3. $W_{bank} = 0.0837 \times W_w + 0.328$

Where W_{bar} is the bar width, W_{bank} is the bank width, and W_w is the predicted stream segment wetted width. Mainstem habitat area not encompassed by bank and bar area was considered to be mid-channel area, which is not preferred habitat by salmon parr, and receives a unique density during fish capacity estimation.

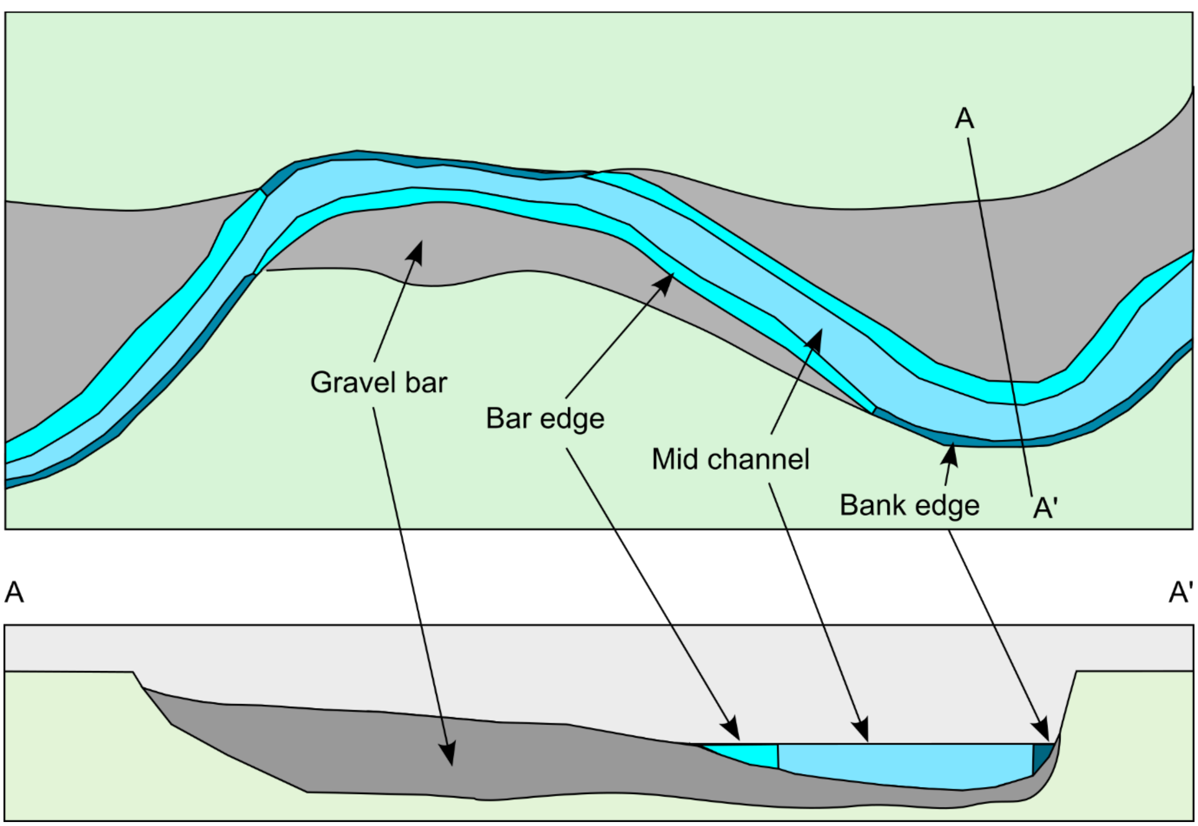

Figure 4. Diagram of large river habitat types in plan view (upper panel) and cross section view (lower panel). Based on Beechie et al. (2005). See also detailed description of unit types in Table 1.

Habitat Modeling – Satellite Image Analysis

In the geomorphic approach, estimates of off-channel habitat are derived from a Columbia River basin-wide model of side channel habitat availability (Bond et al. 2019). However, this model estimates a single value of average annual side channel habitat for each 200 m stream reach, while the actual availability of side channel habitats may vary substantially seasonally. Although we improved estimates of stream gradient and floodplain width (both key attributes in the side channel model) for larger Similkameen River tributaries with 1 m resolution LiDAR data, our estimates continue to lack the context of varying flow. Therefore, to better account for seasonal changes and all types of floodplain habitats (e.g., oxbows, alcoves, beaver ponds, flooded meadows, etc.), we instead estimated a flow-specific wetted habitat area from analysis of a time series of satellite imagery. To do so, we estimated the wetted habitat area in the floodplain of each satellite image, and matched those data with estimates of streamflow at the time of each image capture. The resulting relationship was used to estimate the amount of wetted habitat area across the entire river at a common flow of interest.

High resolution satellite-derived imagery is available for much of the Similkameen River Basin. For our analysis, we focused on imagery from two satellites, Worldview-2 and Worldview-3 (Maxar Technologies, Westminster, CO.). These satellites both provide nine spectral bands of interest for image analysis. In particular, there are eight bands between the wavelengths of 400 and 1040 nm, and each satellite has a panchromatic band of 450-800 nm. Where the two satellites differ substantially is the spatial resolution of each band. At nadir (i.e., imaging an area directly below the satellite), Worldview-3 imagery has a higher resolution at all bands than Worldview-2 imagery (Table 2).

Table 2. The bands, wavelengths assessed in each band, and spatial resolution at nadir for each satellite whose imagery is used in habitat analyses. Resolution decreases as the off-nadir angle increases.

Band	Wavelength range	Worldview-2 resolution	Worldview-3 resolution
Coastal blue	400-450 nm	1.80 m	1.24 m
Blue	450-510 nm	1.80 m	1.24 m
Green	510-580 nm	1.80 m	1.24 m
Yellow	685-625 nm	1.80 m	1.24 m
Red	630-690 nm	1.80 m	1.24 m
Red-Edge	705-745 nm	1.80 m	1.24 m

Near Infrared 1	770-895 nm	1.80 m	1.24 m
Near infrared 2	860-1040 nm	1.80 m	1.24 m
Panchromatic	450-800 nm	0.46 m	0.30 m

Satellite imagery was collected from Maxar's Global Enhanced Geospatial Intelligence Delivery service (www.evwhs.digitalglobe.com), and delivered as zipped GeoTIFF files of level 1b imagery. Level 1b imagery (i.e., "basic all bands") is uncalibrated, unorthorectified imagery of digital numbers (DNs). We used ENVI geospatial software version 5.6.2 (Exelis Visual Information Solutions, Boulder, Colorado) to prepare this imagery for analysis of the water area. First, we performed radiometric calibration to top-of-atmosphere reflectance. Each calibrated image was orthorectified with a digital elevation model (DEM) of the basin compiled from U.S. (10 m resolution) and upsampled Canadian (20 m resolution) sources (Beechie and Imaki 2014). We created 8 spectral indices: the Green Normalized Difference Vegetation Index (GNDVI), the Normalized Difference Vegetation Index (NDVI), the Worldview Built-up Index (WVBI), the Worldview Improved Vegetative Index (WVVI), the Worldview New Iron Index (WVII), the Worldview Soil Index (WVSI), and the Worldview Water Index (WVWI). Each of these spectral indices is defined by the following equations:

$$Eq. 4: GNDVI = \frac{(NIR - Green)}{(NIR + Green)}$$

$$Eq. 5: NDVI = \frac{(NIR - Red)}{(NIR + Red)}$$

$$Eq. 6: GNDVI = \frac{(NIR - Green)}{(NIR + Green)}$$

$$Eq. 7: WVBI = \frac{(Coastal - Red\_Edge)}{(Coastal + Red\_Edge)}$$

$$Eq. 8: WVVI = \frac{(NIR2 - Red)}{(NIR2 + Red)}$$

$$Eq. 9: WVII = \frac{(Green * Yellow)}{(Blue * 1000)}$$

$$Eq. 10: WVSI = \frac{(Green - Yellow)}{(Green + Yellow)}$$

$$Eq. 11: WVWI = \frac{(Coastal - NIR2)}{(Coastal + NIR2)}$$

For each image scene, a composite 17-band, calibrated, orthorectified image was created by combining each original multispectral band, the panchromatic band, and the eight derived indices. This final composite was resampled (nearest neighbor) to the pixel size of the high resolution panchromatic band (~0.3-0.6 m), but lower resolution bands were not pan-sharpened.

To estimate the wetted area of each 17-band composite, we iteratively trained a convolutional neural network (CNN) with the ENVI Deep Learning Module version 1.2.0. For classifying large amounts of imagery with billions of pixels, a classifier needs to not only have a high precision and recall, but also rapid prediction. CNNs have become a standard resource for classifying imagery with complex input data (spectral, shape, context). With high powered graphics processing units, classification of imagery with CNNs is both faster and provides better prediction on novel data than other machine learning methods we have tested with these data that classify each pixel separately (e.g., random forest, support vector machines). Initial training data were created in Esri ArcGIS Pro (Environmental Systems Research Institute, Redlands, CA), version 2.7.0, by hand digitizing shapefiles indicating which pixels in a training image were water. CNN models were trained for 30 epochs, with 2 patches per batch and 1300 batches per epoch. To augment training data and increase model recognition of water, patches were randomly rotated, the loss parameter was set to 0, and a class weight minimum of 1 and maximum of 3 were used. 85% of the input data were used for model training and 15% for model validation. After training, the model with the highest F1 score (weighted average of precision and recall) was used to predict the water area in a new training image. Following prediction, the predicted water area was hand edited to remove errors or wetted areas that were missed in prediction. The resulting cleaned data was added back to the training dataset, and a new model was trained. This process was repeated, adding new imagery from novel areas and image dates, until there was minimal model improvement and little cleaning of test imagery was needed. In total 31 training images, comprising 50,128,383 water pixels (ca. 12,532,095 m^2), from Worldview-2/3 imagery from various seasons and habitat types were used to train the final model. The final model had a validation F1 score of 0.943 (precision = 0.920, recall = 0.966), indicating a robust classifier.

To define a valley bottom for the mainstem Similkameen River, we created a relative elevation model (REM) following the methods of Olson et al. (2014). First, we created a raster of resampled stream elevations with the available 1 m resolution LiDAR derived elevation data and elevation points every 50 m along a hand digitized river thalweg. The final REM was created by subtracting the resampled stream surface elevation raster from the DEM, resulting in relative elevations from the stream surface along its length. To estimate the valley bottom area, we digitally filled the REM to a depth of 4.7 m, which best matched a visual assessment of the valley bottom. The resulting area was clipped to remove areas that are currently separated from the natural valley bottom by roads. The valley bottom raster was split using a cost allocation procedure in ArcGIS Pro to allocate a portion of the valley bottom to each 200 m stream segment. Although the parsimonious assignment of the valley bottom to each stream segment results in segments receiving different valley bottom areas, the resulting polygons are a standard frame of reference to track a common location across imagery of differing flows.

In a similar procedure to estimating valley bottom areas, a mainstem Similkameen River bankfull width raster was created by filling the REM to a depth of 0.53 m, which best matched a visual assessment of bankfull area from satellite imagery. Floodplain habitat depicted as inundated at this fill depth was manually removed to ensure the estimated area only included mainstem habitat. The mainstem bankfull width raster was converted to a polygon and clipped to the valley bottom polygon for each 200 m stream segment to complete the estimate of mainstem bankfull area and the estimate of valley bottom area for each 200 m stream segment. Therefore, satellite image predicted wetted area in excess of the bankfull width stream extent was assumed to be floodplain habitat.

Sixteen Worldview-2/3 images (2011-2022) were classified to assess all inundated areas in each image that overlapped with the LiDAR-derived valley bottom in the mainstem Similkameen River. The resulting classification was converted to a polygon, clipped to the valley bottom for each 200 m stream segment, and the area of wetted floodplain was noted. To estimate the streamflow for each satellite image date and time, we used the mainstem Similkameen River discharge near Hedley, BC (https://wateroffice.ec.gc.ca/report/real_time_e.html?stn=08NL038). For each stream segment we estimated the relationship between discharge and wetted floodplain habitat area as a linear interpolation between each discharge-area point. From this relationship, we estimated the floodplain habitat area at two streamflows across the mainstem Similkameen: 10 $m^3 \cdot s^{-1}$, which is the approximate average flow on August 31 when spring-run Chinook salmon would be expected to peak in spawning activity, and 80 $m^3 \cdot s^{-1}$ (Figure 5), which is the average spring flow when emergent fry would benefit from access to off channel habitat in the mainstem. These satellite image based estimates replaced the side channel estimates made from the Columbia River basin-wide geomorphological model. Areas that did not have adequate satellite imagery or REM data retained the original geomorphological estimates. Additionally, we updated bankfull widths for steam segments overlapping the REM by dividing the bankfull area by the stream segment length (in most cases 200 m) to estimate the average width. Floodplain habitat estimates and bankfull widths were updated using satellite derived data for 184 km of the mainstem Similkameen River, primarily between Palmer Lake and Princeton.

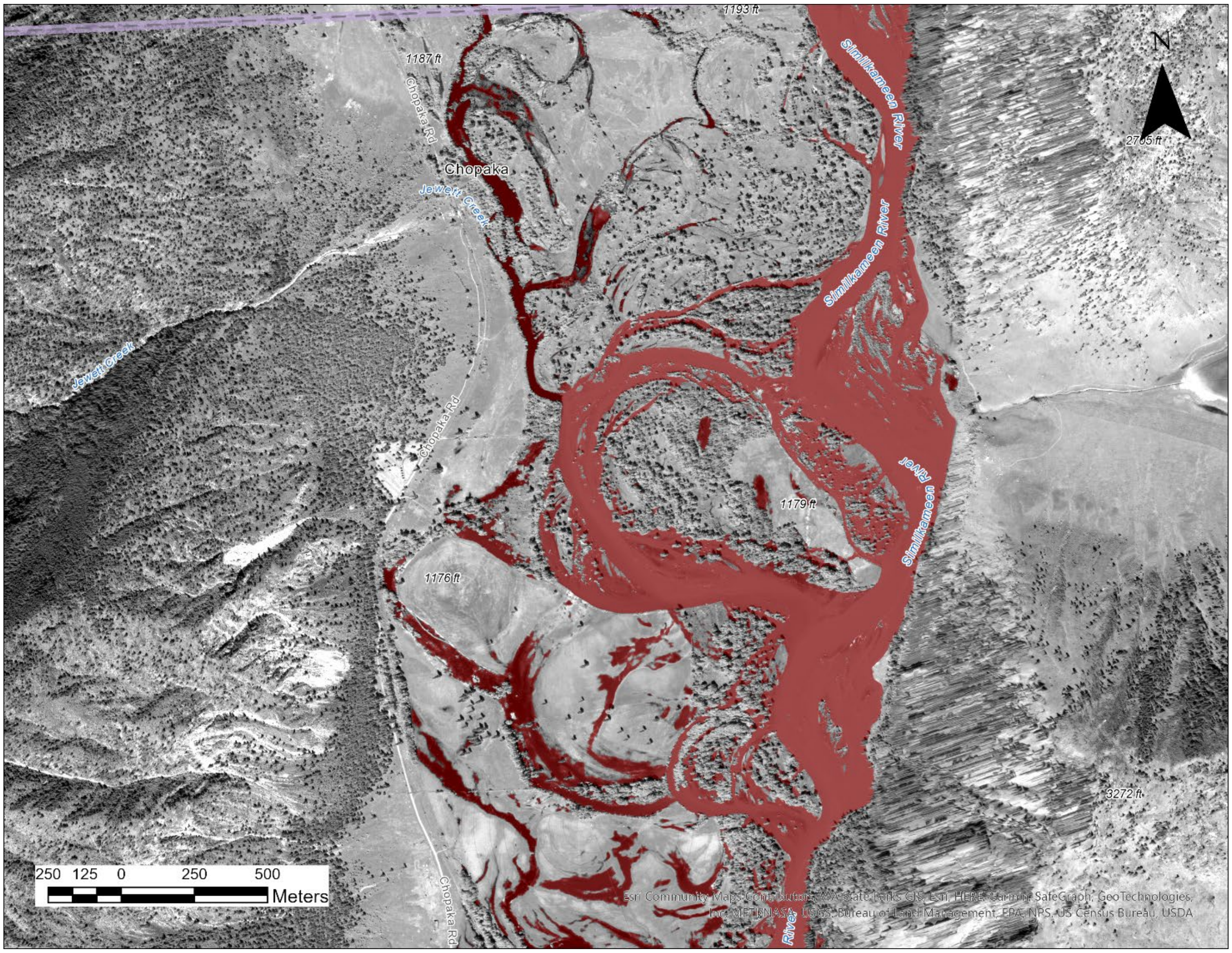

Figure 5. Example of water classification from Worldview 2 imagery of the lower Similkameen River valley bottom during high flow condition (ca. 80 $m^3 \cdot s^{-1}$). Red shaded areas indicate predicted surface water displayed over the panchromatic band.

Juvenile (parr) rearing capacity estimation

After habitat unit areas were estimated, we applied capacity parr densities to each distinct habitat unit (Table 3) and then summed across all unit types to estimate reach- and basin-scale habitat capacities (Figures 6 and 7).

Table 3. Parr capacity densities applied to each estimated habitat type.

Macro habitat type	Habitat type	Chinook parr density (fish/m²)	Steelhead parr density (fish/m²)
Small stream	Riffle	0.02	0.53
	Pool	0.05	0.70
Large river	Bank edge	1.27	1.27
	Bar edge	0.64	1.59
	Mid-channel	0.001	0.064
Floodplain	Side Channel	1.27	0.60

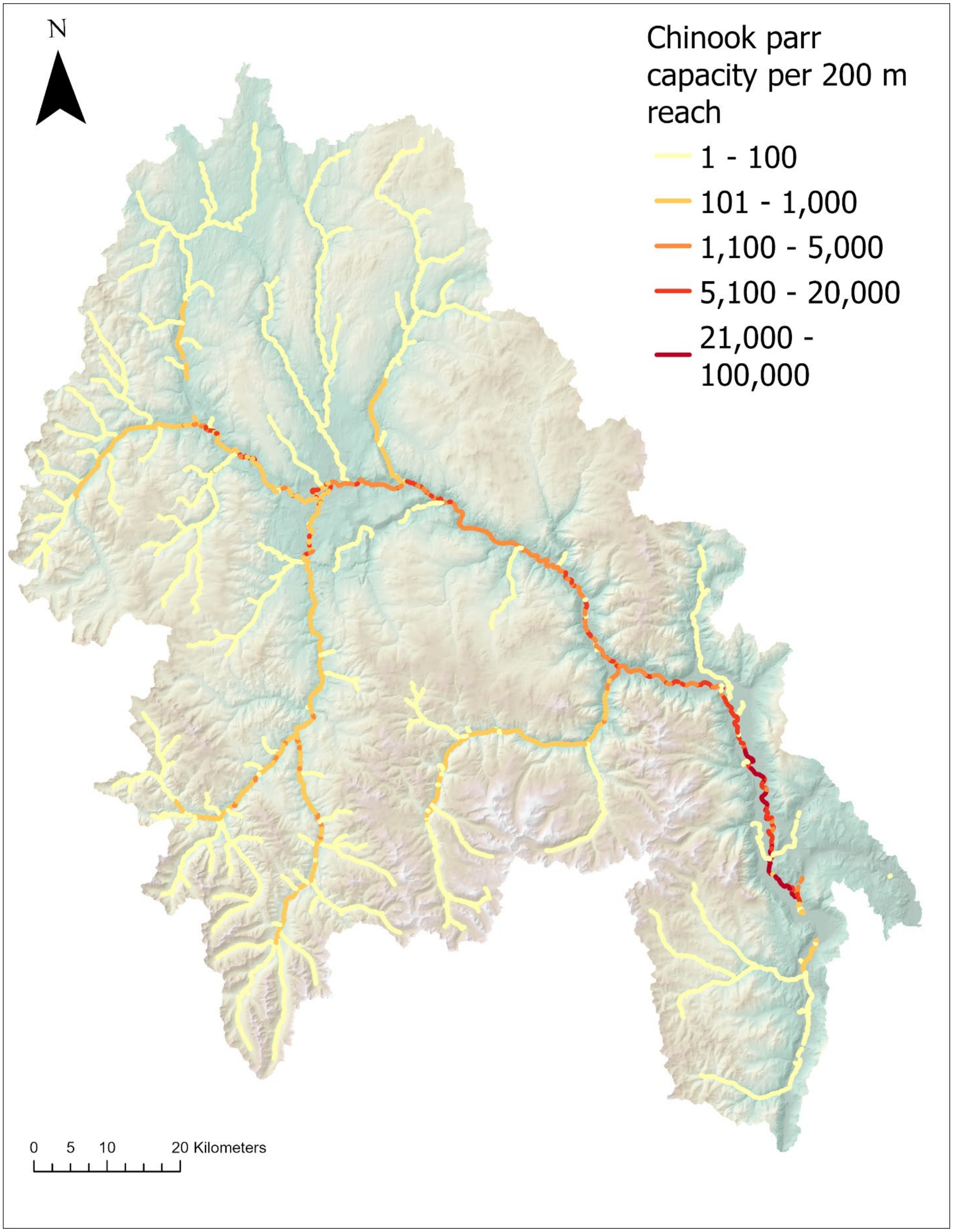

Figure 6. Chinook salmon parr capacity by reach for the estimated anadromous extent. Color scale indicates total capacity for each reach in number of parr.

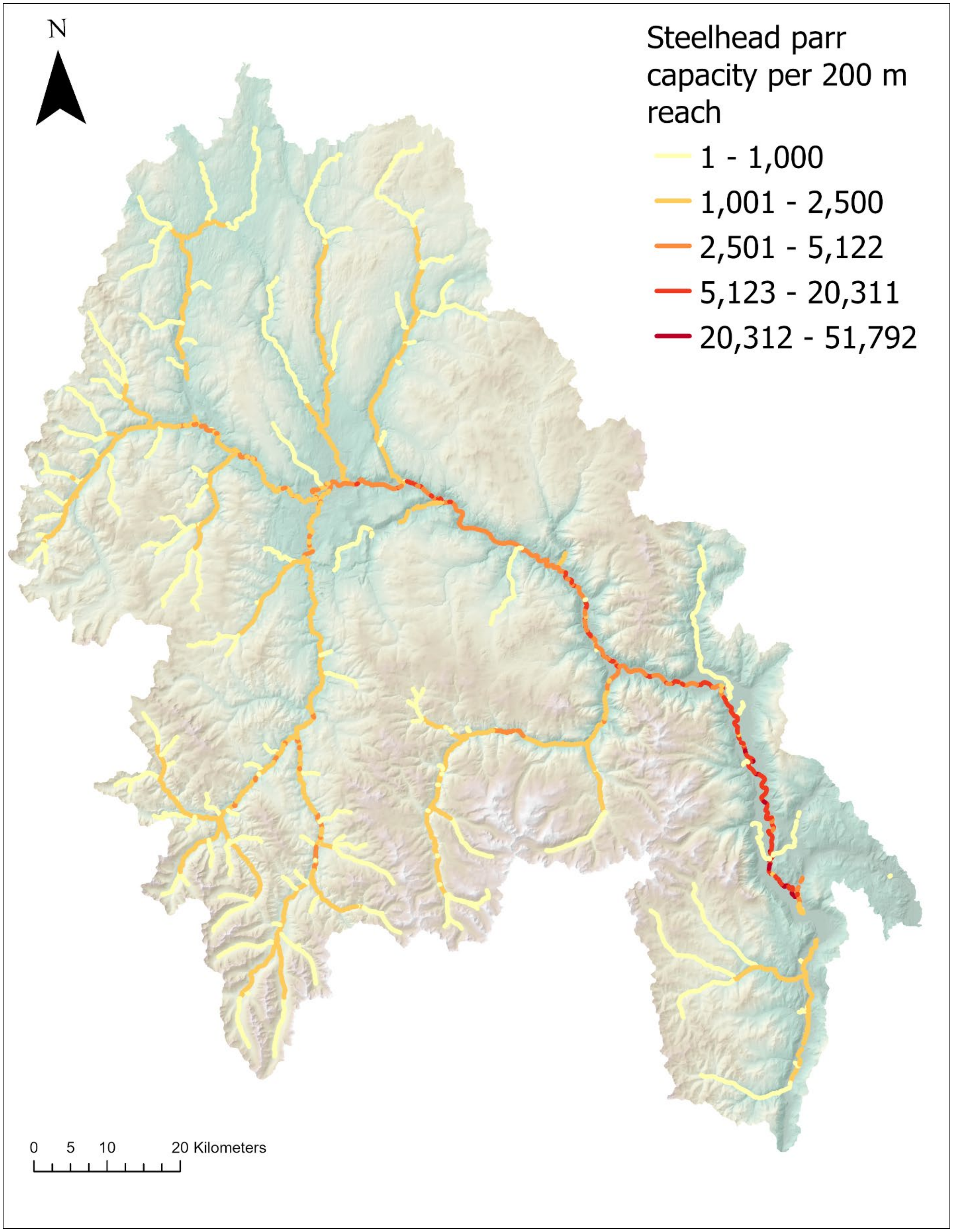

Figure 7. Steelhead parr capacity by reach for the estimated anadromous extent. Color scale indicates total capacity for each 200m reach in number of parr.

Spawning capacity estimation

The spawning capacity for each reach was estimated using the previously derived habitat characteristics for each reach. In particular, following the methods of Beechie et al. (2021), we estimated the spawnable gravel area for each small stream reach using the following equations:

Eq. 12 Pool Number = reach length / (pool spacing × wetted width)

and

Eq. 13 Spawning Area = Pool Number * wetted width * (wetted width * 0.5)

Pool spacing was determined by slope class. In the summer and fall of 2022, the Lower Similkameen Indian Band (LSIB) biologists surveyed 32 sites throughout the Similkameen basin. Selected sites were stratified by slope class, and surveys measured stream width and the number of pools at near baseflow for reaches of at least ten times the bankfull width. From these data, we found that slopes <1% had an average pool spacing of 5.12 bankfull widths per pool, which is nearly identical to the pool spacing of 5 bankfull widths per pool used in previous estimates of this slope class (Beechie et al. 2021). In contrast, the higher gradient streams (>1%) had denser pool network than expected, 6.59 bankfull widths per pool, compared to the pool spacing of 11 bankfull widths per pool in previous work. We used the locally derived pool density estimates for all streams in the appropriate slope class throughout the basin. For each species we assumed a minimum stream size of 3.6 m bankfull width for spawning habitat (Cooney and Holzer 2006).

Large stream (>20 m BFW) spawning gravel was estimated by confinement class. Spawning gravel percentages of area were derived from measurements in post-glacial valleys in the Skagit and Stillaguamish River basins. For confined streams (valley width/bfw ≤ 4), we assume the percent spawning gravel is 3.4%, while in unconfined reaches (valley width/bfw >4) spawning gravels were estimated at 5.5% of total area. To estimate spawning capacity, we divided total estimated spawning area in each reach by the average redd size for each species. We assumed an average redd size of 5.4 m^2 (Orcutt et al. 1968) for steelhead, and 14.1 m^2 for Chinook salmon (Beechie et al. 2006). Spatial depiction of the resulting reach-specific redd capacity is provided on Figures 8 and 9.

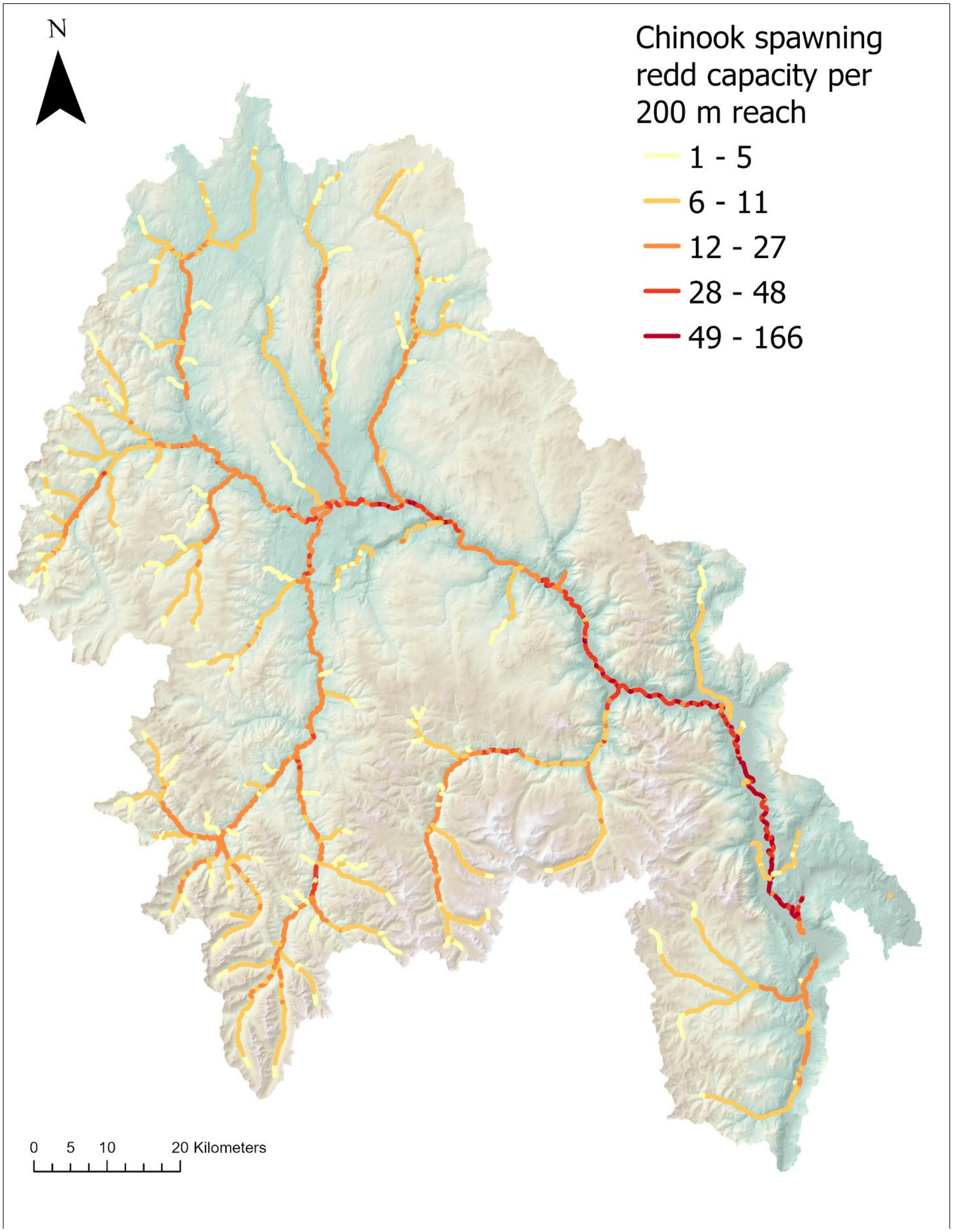

Figure 8. Chinook redd capacity by reach for the estimated anadromous extent. Color scale indicates total redd capacity with each reach colored separately.

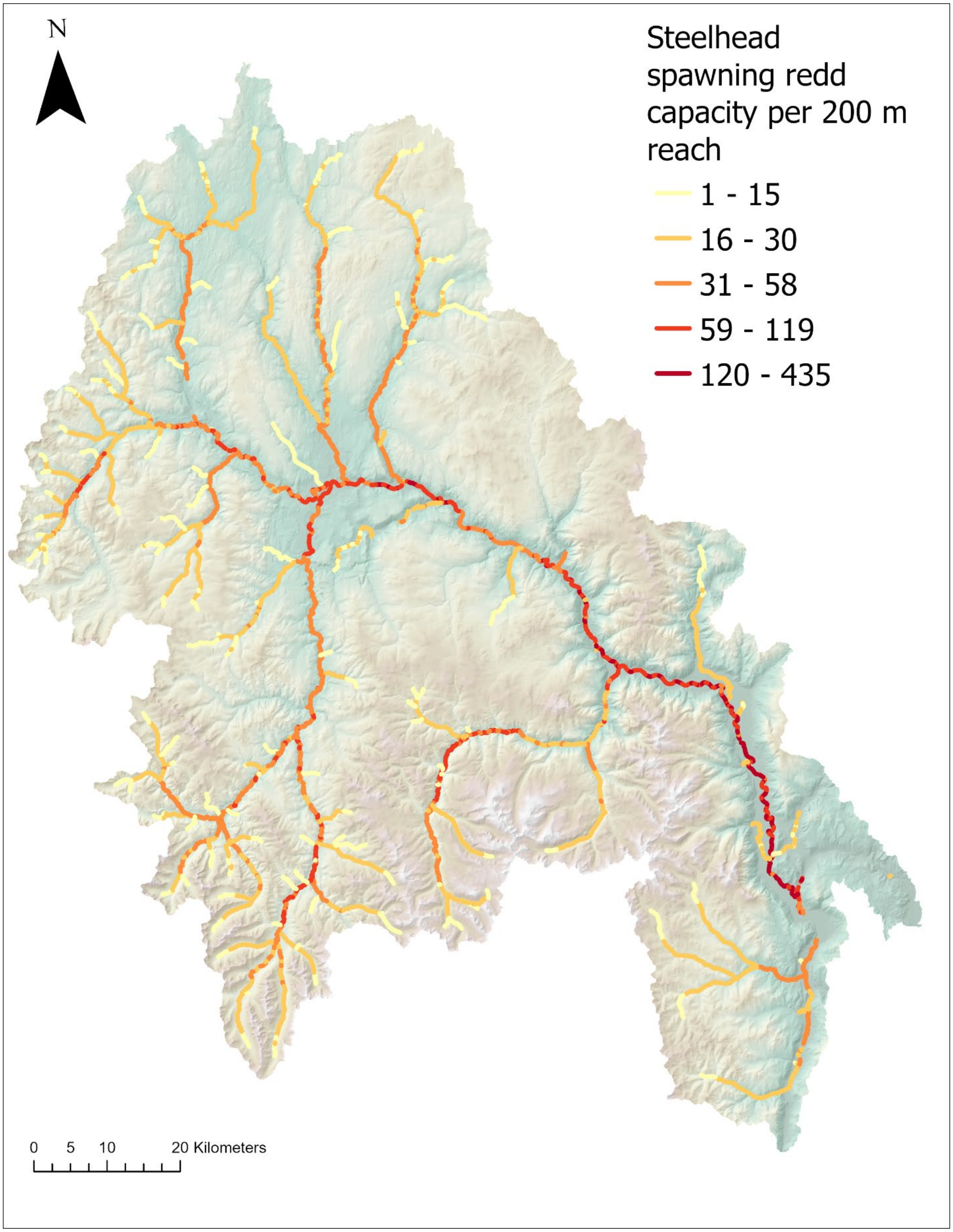

Figure 9. Steelhead redd capacity by reach for the estimated anadromous extent. Color scale indicates total redd capacity with each reach colored separately.

Watershed-specific results

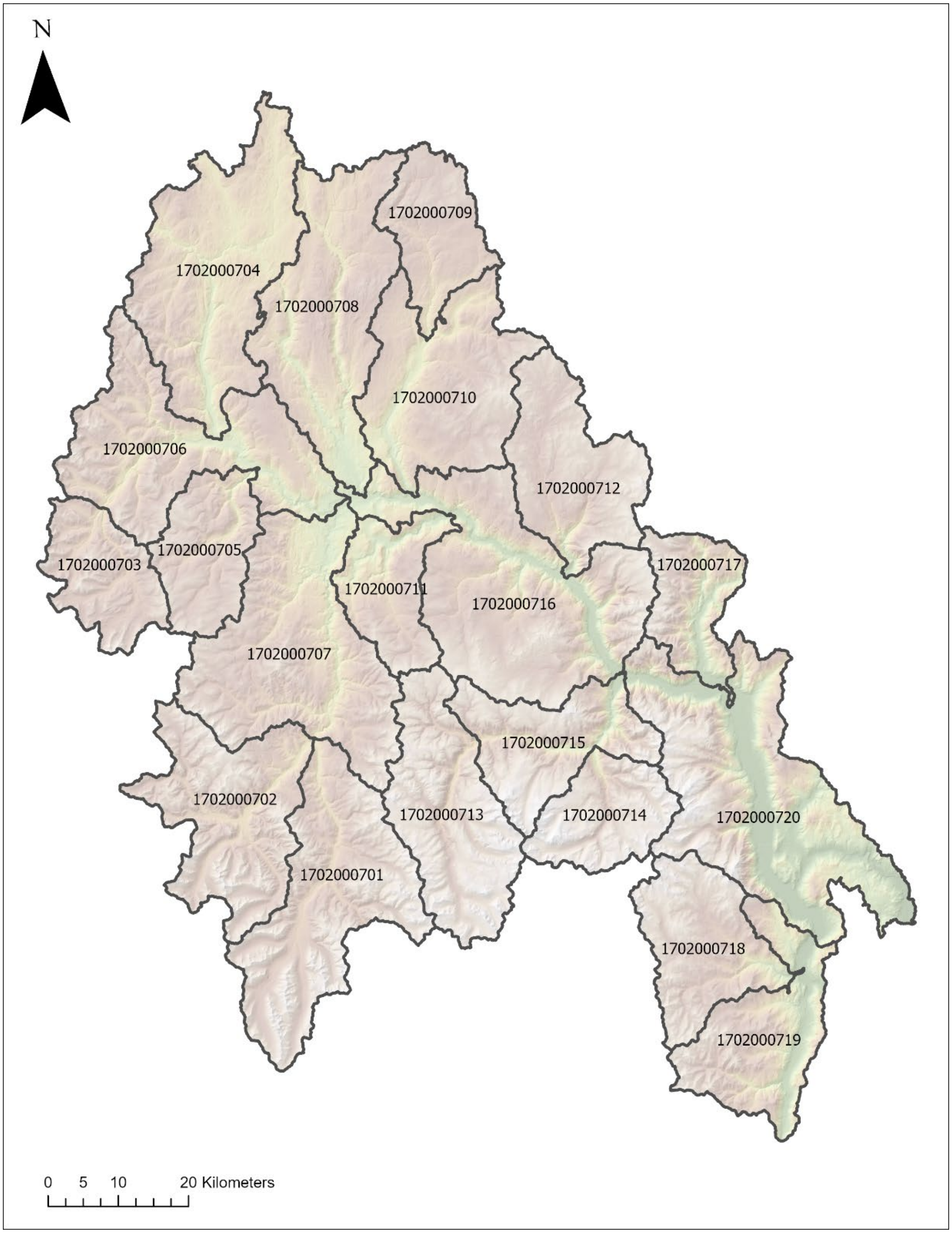

Figure 10. The Similkameen River watershed with ten digit Hydrologic Unit Codes used to identify individual regions (watersheds), delineated in Table 4.

Table 4. Redd and parr capacities for Chinook salmon and steelhead summed by 10 digit hydrologic unit code (USGS, Figure 10). Watersheds that occur in the US use the USGS naming code for basins. There is no USGS naming convention for HUC10 watersheds that occur solely in Canada, so those are named by their primary tributary name.

HUC10	Basin Name	Chinook Salmon redds	Steelhead redds	Chinook salmon parr	Steelhead parr
1702000702	Castle Creek-Similkameen River	7,019	18,327	139,871	768,158
1702000703	Tulameen River/Vuich Creek	1,124	2,935	7,471	123,336
1702000704	Otter Creek	4,940	12,900	30,532	487,497
1702000705	Granite Creek	2,664	6,956	17,369	292,446
1702000706	Tulameen River	8,320	21,724	371,752	1,004,418
1702000707	Similkameen River/Whipsaw Creek	5,751	15,017	304,232	738,186
1702000708	Allison Creek	4,755	12,416	29,243	479,838
1702000709	Siwash Creek	1,717	4,483	11,336	181,224
1702000710	Hayes Creek	3,271	8,540	19,990	333,039
1702000711	Wolf Creek	654	1,709	4,065	69,516
1702000712	McNulty Creek	147	383	949	16,212
1702000716	Similkameen River (Ashnola R. to Princeton)	9,956	25,996	918,315	1,212,659
1702000717	Olalla River	1,039	2,714	6,497	112,692
1702000718	Toats Coulee Creek	2,244	5,860	13,519	247,315
1702000719	Sinlahekin Creek	2,458	6,419	14,372	243,793
1702000720	Snehumption Creek-Similkameen River (Okanogan R. confluence to Ashanola R.)	16,567	43,258	4,602,627	3,076,063
	Totals (all HUC's combined)	72,627	189,637	6,492,139	9,386,391

Discussion

With a watershed area nearly twice the size of the Methow River, the Similkameen River basin represents a substantial amount of potential anadromous salmonid habitat above the Enloe Dam site. Although there are some formidable barriers that block access to portions of the system (e.g., Tulameen Falls), much of the basin would be readily accessible to fishes ascending past the Enloe Dam location. Estimates of spawner capacity from this study are similar to previous estimates of capacity for the Similkameen River Basin based on extensive ground surveys in the early 1980s. A Department of Energy (1984) study previously estimated spawning capacities of steelhead (98,000) and Chinook salmon (55,000) that are broadly similar to our estimates of 189,637 and 72,627 respectively. Their study, however, did not estimate parr, but rather smolt production. To compare our results to that work, we have applied some assumptions about steelhead and Chinook salmon parr to smolt survival (Table 5) derived from other Upper Columbia River populations. The DoE study estimated smolt production for steelhead at 610,000, while our parr estimates converted to smolts through a parr-to-smolt survival proportion of 0.4 (Dan Rawding, WDFW, pers. comm.), would be closer to 2.8 million. The DoE study also estimated Chinook smolt capacity at 1.6-4.8 million, which is similar to our estimate of 2.5 million through a parr to smolt survival proportion of 0.3 (Dan Rawding, WDFW, pers. comm.).

In this study we relied on remotely sensed delineation of migration barriers, documented substantial barriers (e.g., waterfalls), and recent (2021) ground survey data by Upper and Lower Similkameen Bands Tribal Biologists. In some cases, the ground survey data noted barriers not detected by elevation data alone. However, in several cases, the ground surveys indicated that logjams were forming barriers. We did not explicitly

Table 5. Exploration of potential adult returns from full-seeding parr capacity estimates of Chinook salmon and steelhead and contemporary survival estimates from parr-to-smolt and smolt-to-adult stages. Survivals are average estimates from a preliminary analysis by Dan Rawding (WDFW, pers. comm.) using PIT tag mark-recapture analysis in nearby watersheds (Okanogan R., Methow R., Entiat R., Wenatchee R.).

Species	Estimated parr capacity	Average parr-to-smolt survival (proportion)	Smolts	Smolt-to-adult survival (low, proportion)	Smolt-to-adult survival (high, proportion)	Returning adults
Chinook salmon	6,492,139	0.4	2,596,856	0.005	0.03	12,984-77,905
Steelhead	9,386,391	0.3	2,815,917	0.01	0.04	28,159-112,636

exclude areas above logjams unless they were also indicated as a barrier by stream gradient. In our previous work, we have found it rare that logjams alone form true barriers for migrating salmon. In addition, the ground surveys were not conducted until late summer, and many tributaries were listed as dry. Although these streams may in fact be too small to support spawning salmon, further spring or early summer surveys are necessary to identify whether these tributaries are unusable, since salmon may spawn in intermittent streams and juveniles may move to larger rivers prior to low flows in the late summer and fall.

In the 1984 DoE report, it was noted that two tributaries have areas of difficult passage for adult salmon ascending the system: the upper Similkameen above Similkameen Falls (primarily the Pasayten River), and the lower Ashnola River, near Keremeos. Although detailed hydraulic studies of both reaches have not been conducted, from photographic evidence, aerial imagery, and site visitation by local biologists (Chris Fisher, Confederated Tribes of the Colville Reservation, personal communication), passage of the Ashnola River appears to be of sufficient difficulty to warrant removal from capacity estimate totals, while the Pasayten was provisionally included. Ultimately, a more detailed hydraulic analysis of these areas would determine which flows may inhibit passage and how often those flows are achieved during the typical spawning migration period of each species. It may be that each area proves to be impassable in some years, limiting the capacity of the system at times, or they may be functionally impassable at most seasonally important flows.

In addition, we cannot reasonably assess the area directly impounded behind Enloe Dam. We did not attempt to estimate stream characteristics for the confined, sediment-laden impounded area, or what habitat may be available after dam removal. There is currently use of the lower Similkameen River below Enloe Dam for spawning by fall-run Chinook salmon. Although passage at the Enloe Dam site could also allow fall-run Chinook into the currently impounded area above the dam, we do not consider fall-run Chinook habitat or capacity for this study, as the characteristics of the lower Similkameen River would likely change considerably with dam removal and sediment transport, and to our knowledge, no pre-dam data exist about the lower river habitat.

Our estimates of capacity are heavily dependent upon pool spacing data, which is driven primarily by instream wood load. Our initial modeling estimated wood loads from other nearby streams (e.g., Skagit River). The earlier Department of Energy (1984) study mentions measuring wood in reach surveys, but provides no estimates of wood in their report. From similar work in Puget Sound streams, increasing wood load can change pool spacing considerably. For example, we estimate that for the high slope stream reach class (>1% slope), low wood abundance leads to 11 bankfull widths per pool, while the same slope class would be only 2 bankfull widths per pool at high wood abundance, a large increase in pool habitat. Survey work by the LSIB in the summer of 2022 established the pool spacing for 32 sites throughout the basin. Their estimates indicated a more dense pool network than our conservative low wood condition (11 bankfull widths per pool). A measured average pool spacing of 6.59 bankfull widths per pool indicates there is likely a higher wood load in the higher gradient reaches of the stream than we originally anticipated, which may have ancillary benefits for spawners and rearing fish in the system.

Although similar geomorphic analyses have been used in various systems in the Pacific Northwest to estimate spawning and rearing capacity, data limitations mean that there are important aspects of the habitat that we cannot assess with this study and it could benefit from more detailed analyses. For example, there may be concerns about chemical contaminants (e.g., Copper Mountain Mine), which could influence survival, but would require water sampling as part of ground surveys. Similarly, a temperature analysis could help inform pre-spawn mortality, a significant source of mortality in other parts of the Columbia River Basin (Bowerman et al. 2021; Jorgensen et al. 2009; Quinn et al. 2007), but was not included in this analysis. We also have not modeled other specific sources of habitat degradation that could be modeled with more data. For example, unpaved road density could provide an estimate of fine sediment, which has implications for embryo survival.

The overall Similkameen River basin system's rearing and spawning capacity is heavily influenced by the mainstem Similkameen River between Palmer Lake and the confluence with the Ashnola River. In that reach of the river, our analysis of satellite imagery indicated substantially more inundated floodplain habitat at both low and high flows than predicted from the geomorphic model. This habitat likely provides a diverse suite of habitats supporting refuge from predation and high flows as well as food resources for rearing juveniles. Although analysis of the satellite imagery provides a quantitative assessment of the wetted habitat area, estimating the connectivity of those habitats with mainstem and side channel areas would require a more detailed hydraulic model or ground surveys. Therefore, some habitats, although forming wetted floodplain areas, may not provide a direct benefit to salmon. However, even if some floodplain habitats do not have surface connectivity accessible to fish from the mainstem, these lateral wetlands are likely contributing to the overall productivity of the system by providing invertebrates, nutrients, and diverse thermal environments to accessible areas.

To further identify the potential limiting factors for an anadromous population of Chinook salmon or steelhead in the Similkameen River system, a life cycle approach could be used to bring together estimates of habitat, fish production, and restoration under a common framework. In a life cycle modeling context, alternative scenarios of restoration, instream or en-route survival, as well as production and capacity, could be analyzed to determine which specific habitat actions may benefit these populations or promote their establishment (Honea et al. 2009; Jorgensen et al. 2021).

Literature Cited

Bartz, K. K., and coauthors. 2006. Translating restoration scenarios into habitat conditions: an initial step in evaluating recovery strategies for Chinook salmon (Oncorhynchus tshawytscha). Canadian Journal of Fisheries and Aquatic Sciences 63(7):1578-1595.

Beechie, T., and H. Imaki. 2014. Predicting natural channel patterns based on landscape and geomorphic controls in the Columbia River basin, USA. Water Resources Research 50(1):39-57.

Beechie, T., E. Beamer, and L. Wasserman. 1994. Estimating coho salmon rearing habitat and smolt production losses in a large river basin, and implications for habitat restoration. North American Journal of Fisheries Management 14(4):797-811.

Beechie, T. J., B. D. Collins, and G. R. Pess. 2001. Holocene and recent geomorphic processes, land use, and salmonid habitat in two north Puget Sound river basins. Geomorphic processes and riverine habitat, Water Science and Application 4:37-54.

Beechie, T. J., C. Fogel, C. Nicol, and B. Timpane-Padgham. 2021. A process-based assessment of landscape change and salmon habitat losses in the Chehalis River basin, USA. Plos One 16(11).

Beechie, T. J., C. M. Greene, L. Holsinger, and E. M. Beamer. 2006. Incorporating parameter uncertainty into evaluation of spawning habitat limitations on Chinook salmon (*Oncorhynchus tshawytscha*) populations. Canadian Journal of Fisheries and Aquatic Sciences 63(6):1242-1250.

Beechie, T.J., M. Liermann, E.M. Beamer, and R. Henderson. 2005. A classification of habitat types in a large river and their use by juvenile salmonids. Transactions of the American Fisheries Society 134:717-729.

Bond, M. H., T. G. Nodine, T. Beechie, and R. W. Zabel. 2017. A habitat expansion approach to estimating parr rearing capacity of spring and summer Chinook in the Columbia River Basin. Zabel, Cooney, and Jordan, editor Interior Columbia Basin life-cycle modeling. NWFSC Draft Report, Seattle, WA.

Bond, M. H., T. G. Nodine, T. J. Beechie, and R. W. Zabel. 2019. Estimating the benefits of widespread floodplain reconnection for Columbia River Chinook salmon. Canadian Journal of Fisheries and Aquatic Sciences 76(7):1212-1226.

Bowerman, T. E., M. L. Keefer, and C. C. Caudill. 2021. Elevated stream temperature, origin, and individual size influence Chinook salmon prespawn mortality across the Columbia River Basin. Fisheries Research 237:105874.

Cooney, T., and D. M. Holzer. 2006. Appendix C: Interior Columbia Basin Stream Type Chinook Salmon and Steelhead Populations: Habitat Intrinsic Potential Analysis. ICTRT Viability Criteria Review Draft. Northwest Fisheries Science Center, Seattle WA.

DoE. 1984. Similkameen River habitat inventory. Department of Energy, Bonneville Power Administration, Division of Fish and Wildlife.

Honea, J. M., and coauthors. 2009. Evaluating habitat effects on population status: influence of habitat restoration on spring-run Chinook salmon. Freshwater Biology 54(7):1576-1592.

Jorgensen, J. C., and coauthors. 2009. Linking landscape-level change to habitat quality: an evaluation of restoration actions on the freshwater habitat of spring-run Chinook salmon. Freshwater Biology 54(7):1560-1575.

Jorgensen, J. C., C. Nicol, C. Fogel, and T. J. Beechie. 2021. Identifying the potential of anadromous salmonid habitat restoration with life cycle models. Plos One 16(9):e0256792.

Olson, P. L., Legg, N. T., Abbe, T. B., Reinhart, M. A., and J. K. Radloff. 2014, A Methodology for Delineating Planning-Level Channel Migration Zones: Washington State Department of Ecology Publication no. 14-06-025, 83p.

Orcutt, D. R., B. R. Pulliam, and A. Arp. 1968. Characteristics of Steelhead Trout Redds in Idaho Streams. Transactions of the American Fisheries Society 97(1):42-&.

Quinn, T. P., D. M. Eggers, J. H. Clark, and H. B. Rich. 2007. Density, climate, and the processes of prespawning mortality and egg retention in Pacific salmon (Oncorhynchus spp.). Canadian Journal of Fisheries and Aquatic Sciences 64(3):574-582.

U.S. Secretary of Commerce
Gina M. Raimondo

Under Secretary of Commerce for Oceans and Atmosphere
Dr. Richard W. Spinrad

Assistant Administrator for Fisheries
Janet Coit

January 2023

fisheries.noaa.gov

OFFICIAL BUSINESS

National Marine Fisheries Service
Northwest Fisheries Science Center
2725 Montlake Boulevard East
Seattle, Washington 98112